EPJ manuscript No.
(will be inserted by the editor)

Interpretation of $K^+\bar{K}^0$ pair production in pp collisions

A. Dzyuba[1,2], M.Büscher[1], C. Hanhart[1], V. Kleber[3], V. Koptev[2], H. Ströher[1], and C. Wilkin[4a]

[1] Institut für Kernphysik, Forschungszentrum Jülich, 52425 Jülich, Germany
[2] Petersburg Nuclear Physics Institute, 188300 Gatchina, Russia
[3] Physikalisches Institut, Universität Bonn, 53115 Bonn, Germany
[4] Physics and Astronomy Department, UCL, London WC1E 6BT, UK

Received: February 24, 2013

Abstract. A combined analysis of the published data on the $pp \to dK^+\bar{K}^0$ reaction at excess energies of 47.4 MeV and 104.7 MeV is presented. Evidence is found for both the production of the $a_0^+(980)$ scalar resonance and for a strong $\bar{K}^0 d$ final state interaction.

PACS. 13.60.Le Meson production – 13.75.Jz Kaon-baryon interactions – 14.40.Cs Other mesons with $S = C = 0$, mass < 2.5 GeV

1 Introduction

The nature of the light scalar resonances $a_0(980)$ and $f_0(980)$ is still far from being understood [1]. One reason for this is the lack of precise information about their coupling to the hadronic channels and especially to the $K\bar{K}$ final states [2]. It has been argued that the knowledge of the couplings might allow one to establish whether these light scalars are genuine $q\bar{q}$-mesons, or four-quark, or molecular states [3,4]. In the case of the $a_0(980)$ resonance, many precise measurements have been performed to explore the $\pi\eta$-channel. On the other hand, the data available for the $K\bar{K}$ channel are quite limited, with large statistical errors and poor mass resolution. Further experimental data are therefore necessary in order to clarify the current situation and this was the motivation for the study of $a_0^+(980)$ production in the $pp \to da_0^+ \to dK^+\bar{K}^0$ reaction.

However, kaon pairs can also be created through the $pp \to K^+pY^{0*}$ reaction, where the hyperon decays *via* $Y^* \to \bar{K}^0 n$. A final state interaction between the produced neutron and proton can then lead to the deuteron observed in the $pp \to dK^+\bar{K}^0$ reaction. There are, of course, several excited hyperons that could contribute to such a process. Of particular interest for low energy production are the $\Sigma(1385)$ and the $\Lambda(1405)$. Although the central values of their masses are below the $\bar{K}N$ threshold, their widths extend well above, and these hyperons will certainly influence spectra through a $\bar{K}N$ final state interaction.

There is an extensive program at the COSY COoler SYnchrotron of the Forschungszentrum Jülich to study the production of the $a_0(980)$ and $f_0(980)$ resonances, as well as the $\Sigma(1385)$ and $\Lambda(1405)$ hyperons, in nucleon-nucleon collisions. Using the ANKE magnetic spectrometer and its associated detector systems, placed at an internal target position of the storage ring, positive kaons can be identified against a very high pion and proton background with the help of dedicated ΔE-E telescopes [5]. These allow coincidence measurements with other charged particles to be performed.

The $pp \to dK^+\bar{K}^0$ reaction was investigated at the two proton beam energies of T_p=2.65 GeV [6] and 2.83 GeV [7], corresponding to the excess energies of $\epsilon = 47.4$ MeV and 104.7 MeV, respectively. In both cases the K^+ and the deuteron were measured directly, with the $\bar{K}^0$ being identified through a missing-mass peak.

At energies close to the reaction threshold, only a limited number of partial waves can contribute in the final state. However, conservation laws demand that there be at least one p-wave in the $dK^+\bar{K}^0$ system. This requirement can be expressed in one of several different but equivalent coupling schemes. The data analysis presented in Refs. [6,7] considered an s-wave in the $K\bar{K}$ system in association with a p-wave of the deuteron with respect to the meson pair, $\{(K^+\bar{K}^0)_s d\}_p$, and a p-wave $K^+\bar{K}^0$ pair being in an s-wave with respect to the deuteron, *viz.* $\{(K^+\bar{K}^0)_p d\}_s$.

It should be noted that the $a_0^+(980)$ can contribute only to the $\{(K^+\bar{K}^0)_s d\}_p$ configuration, and the separate analyses of the two data sets revealed the dominance of this channel at both energies. However, when these results are transformed into a basis of the type $\{\{\bar{K}^0 d\}_\ell K^+\}_{\ell'}$, it is seen that the $\{\bar{K}^0 d\}$ system is also dominantly in the s-wave, with the K^+ being in the p-wave. This suggests that the data might be influenced simultaneously by the production of the $a_0^+(980)$ and the $\bar{K}^0 d$ final state interaction.

The relationships between the amplitudes and observables in the different coupling schemes are discussed in Sec. 2. A combined fit to the data at the two energies is presented in Sec. 3, where it is assumed that the relative strengths of the amplitudes are constant in Q, apart from the angular momentum factors. It is to be expected that the shapes of the correspond-

[a] email: cw@hep.ucl.ac.uk

ing spectra would be distorted by both the $a_0^+(980)$ resonance, and the $\bar{K}^0 d$ final state interaction and the theoretical forms of these are the subject of Sec. 4. The possible influence of these two distortions on the $pp \to dK^+\bar{K}^0$ data is studied in Sec. 5, where it is suggested that both contribute significantly to the total cross section, though their effects tend largely to mask each other in the $K^+\bar{K}^0$ mass spectrum. On the other hand, the ratio of the $\bar{K}^0 d$ to $K^+ d$ mass distributions seems to depend primarily on the $\bar{K}^0 d$ final state interaction and only weakly on the parameters of the $a_0^+(980)$ resonance. Our conclusions and suggestions for further work are outlined in Sec. 6.

2 Amplitudes and observables

Since the available data [6,7] were taken quite close to threshold, we here analyse them in terms of the lowest allowed partial waves. The application of angular momentum and parity conservation laws, together with the Pauli principle in the initial state, shows that the final particles in the $pp \to dK^+\bar{K}^0$ reaction cannot all be in relative s-states. The first permitted final states are therefore Sp and Ps, where the first label denotes the orbital angular momentum between the $K^+\bar{K}^0$ pair and the second that of the pair relative to the deuteron. In either case the initial pp pair must have spin-one and be in an odd partial wave. The most general form of the reaction amplitudes corresponding to these transitions are then:

$$\begin{aligned}\mathcal{M}_{Sp} &= a_{Sp}(\hat{\boldsymbol{p}}\cdot\boldsymbol{S})(\boldsymbol{k}\cdot\boldsymbol{\epsilon}^\dagger) + b_{Sp}(\hat{\boldsymbol{p}}\cdot\boldsymbol{k})(\boldsymbol{S}\cdot\boldsymbol{\epsilon}^\dagger)\\ &+c_{Sp}(\boldsymbol{k}\cdot\boldsymbol{S})(\hat{\boldsymbol{p}}\cdot\boldsymbol{\epsilon}^\dagger) + d_{Sp}(\hat{\boldsymbol{p}}\cdot\boldsymbol{S})(\hat{\boldsymbol{p}}\cdot\boldsymbol{\epsilon}^\dagger)(\boldsymbol{k}\cdot\hat{\boldsymbol{p}}). \quad (2.1)\\ \mathcal{M}_{Ps} &= a_{Ps}(\hat{\boldsymbol{p}}\cdot\boldsymbol{S})(\boldsymbol{q}\cdot\boldsymbol{\epsilon}^\dagger) + b_{Ps}(\hat{\boldsymbol{p}}\cdot\boldsymbol{q})(\boldsymbol{S}\cdot\boldsymbol{\epsilon}^\dagger)\\ &+c_{Ps}(\boldsymbol{q}\cdot\boldsymbol{S})(\hat{\boldsymbol{p}}\cdot\boldsymbol{\epsilon}^\dagger) + d_{Ps}(\hat{\boldsymbol{p}}\cdot\boldsymbol{S})(\hat{\boldsymbol{p}}\cdot\boldsymbol{\epsilon}^\dagger)(\boldsymbol{q}\cdot\hat{\boldsymbol{p}}). \quad (2.2)\end{aligned}$$

Here $\boldsymbol{q}$ is the relative momentum between the two kaons, $\boldsymbol{k}$ the deuteron cms momentum, and $\hat{\boldsymbol{p}}$ is the unit vector parallel to the beam direction, also in the centre-of-mass system. The polarisation vectors of the initial pp pair and the final deuteron are denoted by $\boldsymbol{S}$ and $\boldsymbol{\epsilon}$, respectively. The two sets of coefficients a, b, c and d are independent complex amplitudes which may, in principle, depend upon the scalar kinematic quantities q^2, k^2, and $\boldsymbol{k}\cdot\boldsymbol{q}$.

Since no spin dependence has yet been measured in the $pp \to dK^+\bar{K}^0$ reaction, the square of the matrix element must be averaged over the initial and summed over the final spins. This leads to an expression in terms of the three-momenta that characterise the system:

$$\begin{aligned}\overline{|\mathcal{M}(\boldsymbol{k},\boldsymbol{q})|^2} &= C_0^k k^2 + C_1(\hat{\boldsymbol{p}}\cdot\boldsymbol{k})^2 + C_0^q q^2 + C_2(\hat{\boldsymbol{p}}\cdot\boldsymbol{q})^2\\ &+ C_3(\boldsymbol{k}\cdot\boldsymbol{q}) + C_4(\hat{\boldsymbol{p}}\cdot\boldsymbol{k})(\hat{\boldsymbol{p}}\cdot\boldsymbol{q})\,. \quad (2.3)\end{aligned}$$

The C-coefficients are bilinear combinations of the amplitudes of Eqs. (2.1) and (2.2) [8]:

$$\begin{aligned}C_0^q &= \tfrac{1}{2}(|a_{Ps}|^2 + |c_{Ps}|^2),\\ C_0^k &= \tfrac{1}{2}(|a_{Sp}|^2 + |c_{Sp}|^2),\\ C_1 &= |b_{Sp}|^2 + \tfrac{1}{2}|b_{Sp}+d_{Sp}|^2\\ &\quad + Re\left\{a_{Sp}^* c_{Sp} + (a_{Sp}+c_{Sp})^*(b_{Sp}+d_{Sp})\right\},\\ C_2 &= |b_{Ps}|^2 + \tfrac{1}{2}|b_{Ps}+d_{Ps}|^2\\ &\quad + Re\left\{a_{Ps}^* c_{Ps} + (a_{Ps}+c_{Ps})^*(b_{Ps}+d_{Ps})\right\},\\ C_3 &= Re\left\{a_{Ps}a_{Sp}^* + c_{Ps}c_{Sp}^*\right\},\\ C_4 &= Re\left\{(a_{Ps}+c_{Ps}+b_{Ps}+d_{Ps})^*\right.\\ &\quad \left.\times(a_{Sp}+c_{Sp}+b_{Sp}+d_{Sp}) + 2b_{Ps}^* b_{Sp})\right\}. \quad (2.4)\end{aligned}$$

It is seen from Eqs. (2.4) that only $K\bar{K}$ p-waves contribute to C_0^q and C_2 and only s-waves to C_0^k and C_1. The coefficients C_3 and C_4 represent the s–p interference terms. In a first approximation it might be assumed that close to threshold the C are constant, and the data were analysed on the basis of this *ansatz* [6,7]. However, whereas the spectra obtained at the two different energies could be fitted well individually, a combined analysis of both data sets was not possible while keeping the assumption that the aforementioned coefficients are constant.

The coefficients C must be such that the absolute square of the matrix element of Eq. (2.3) should not be negative anywhere in the allowed $(\boldsymbol{k},\boldsymbol{q})$ space. In practice it is sufficient to impose the somewhat weaker condition:

$$4(C_0^k + \beta\, C_1)(C_0^q + \beta\, C_2) \geq (C_3 + \beta\, C_4)^2 \quad (2.5)$$

for all β in the range $0 \leq \beta \leq 1$. This positivity requirement was not met by the earlier analyses [6,7].

The presence of the $a_0^+(980)$ could distort the $K^+\bar{K}^0$ s-wave amplitudes of Eq. (2.1) and hence introduce a momentum dependence into some of the C coefficients of Eq. (2.3). However, this basis is not optimal if the variation with momentum is due mainly to a final-state interaction between the $\bar{K}^0$ and the deuteron. For this it is better to couple first the $\bar{K}^0 d$ system, *i.e.* use the basis $\left\{\{\bar{K}^0 d\}_l K^+\right\}_{l'}$. The relationship between the amplitudes in the two bases is easily found by defining $\boldsymbol{Q}$ as the relative $\bar{K}^0 d$ momentum and $\boldsymbol{K}$ as the momentum of the K^+ in the overall cms. Non-relativistically, these are connected to the original momenta through

$$\begin{aligned}\boldsymbol{k} &= \boldsymbol{Q} - \alpha\boldsymbol{K},\\ \boldsymbol{q} &= \left(1 - \tfrac{1}{2}\alpha\right)\boldsymbol{K} + \boldsymbol{Q}, \quad (2.6)\end{aligned}$$

where the kinematic factor $\alpha = m_d/(m_d+m_K)$ depends upon the deuteron and kaon masses [8]. The desired expressions are then found by inserting Eq. (2.6) into Eqs. (2.1) and (2.2).

The spin-averaged matrix element squared has exactly the same general structure as that of Eq. (2.3) but in the new variables:

$$\begin{aligned}\overline{|\mathcal{M}(\boldsymbol{K},\boldsymbol{Q})|^2} &= B_0^K K^2 + B_1(\hat{\boldsymbol{p}}\cdot\boldsymbol{K})^2 + B_0^Q Q^2 + B_2(\hat{\boldsymbol{p}}\cdot\boldsymbol{Q})^2\\ &+ B_3(\boldsymbol{K}\cdot\boldsymbol{Q}) + B_4(\hat{\boldsymbol{p}}\cdot\boldsymbol{K})(\hat{\boldsymbol{p}}\cdot\boldsymbol{Q})\,. \quad (2.7)\end{aligned}$$

The interpretation is also completely analogous, with B_0^K and B_1 representing the $\bar{K}^0 d$ s-waves and B_0^Q and B_2 the p-waves. The transformation of the observables between the two bases is given by

$$\begin{aligned}B_0^Q &= C_0^k + \tfrac{1}{4}C_0^q + \tfrac{1}{2}C_3,\\ B_2 &= C_1 + \tfrac{1}{4}C_2 + \tfrac{1}{2}C_4,\\ B_0^K &= \alpha^2 C_0^k + \tfrac{1}{4}(2-\alpha)^2 C_0^q - \tfrac{1}{2}\alpha(2-\alpha)C_3,\\ B_1 &= \alpha^2 C_1 + \tfrac{1}{4}(2-\alpha)^2 C_2 - \tfrac{1}{2}\alpha(2-\alpha)C_4,\\ B_3 &= -2\alpha C_0^k + \tfrac{1}{2}(2-\alpha)C_0^q + (1-\alpha)C_3,\\ B_4 &= -2\alpha C_1 + \tfrac{1}{2}(2-\alpha)C_2 + (1-\alpha)C_4\,. \quad (2.8)\end{aligned}$$

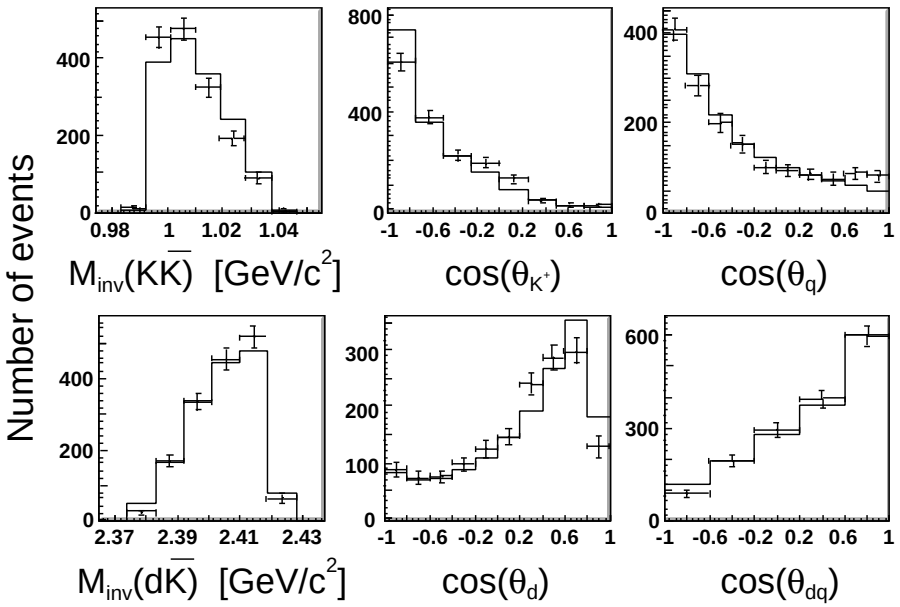

Fig. 1. Best combined fit to the efficiency-corrected numbers of events in the 47.4 MeV data on the basis of the constant amplitude *ansatz* of Eq. (2.3). Here $(\theta_{K^+}, \theta_d, \theta_q)$ are the c.m. angles of the K^+, deuteron, and $K^+\bar{K}^0$ relative momentum with respect to the proton beam direction. The angle between the $K^+\bar{K}^0$ relative momentum and the final deuteron momentum is denoted by θ_{dq}.

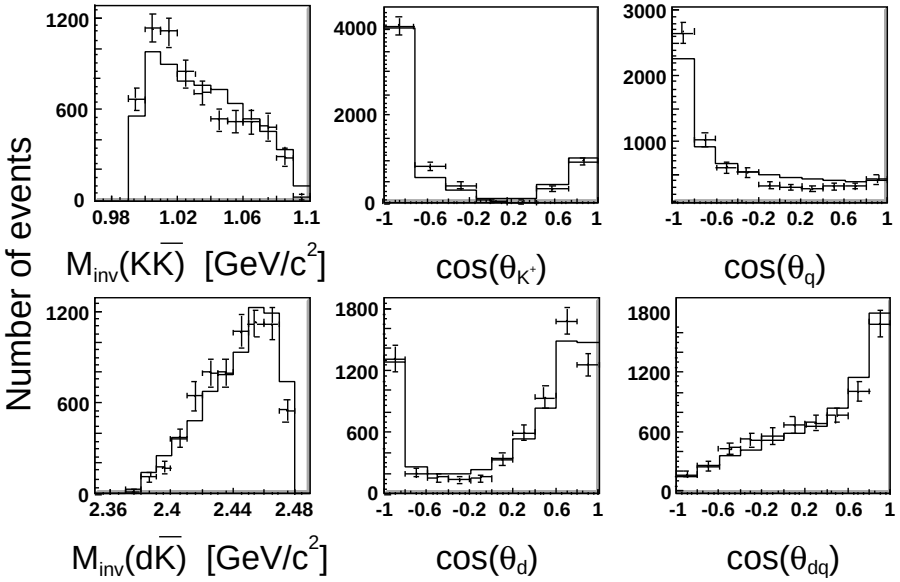

Fig. 2. The same as Fig. 1 for the 104.7 MeV data.

It should be noted that if the positivity conditions of Eq. (2.5) are imposed in the $\{\{\bar{K}^0K^+\}d\}$ basis, they are automatically satisfied in the $\{\{\bar{K}^0d\}K^+\}$ basis, and *vice-versa*.

The amplitudes are normalised such that, for a fixed total c.m. energy $\sqrt{s}$, the total cross section is given by

$$\sigma = \frac{1}{64\pi^3 s\, p_p} \int_{m_1+m_2}^{\sqrt{s}-m_3} p_3\, p_1^*\, \langle\, \overline{|\mathcal{M}^2|}\, \rangle\, \mathrm{d}M_{12}\,, \qquad (2.9)$$

where $\langle\, \overline{|\mathcal{M}^2|}\, \rangle$ is the angular-average of the squared transition matrix element of Eq. (2.3) or (2.7). The momentum p_p of the incident proton and p_3 of particle-3 are evaluated in the overall c.m. frame, while that of particle-1, p_1^*, is considered in the rest frame of the (12) system, where the effective mass is M_{12}.

3 Solutions with constant coefficients

In order to determine the C parameters defined in Eq. (2.3), we performed fits of the measured observables using GEANT simulated data samples. This method, which is described in detail in Ref. [7], works directly with the distributions uncorrected for acceptance, which is then taken into account in the simulation.

The results of making separate single-energy fits, as well as of a combined study of the two energies, are shown in Table 1.

Table 1. Results of the fits to the shapes of the differential distributions on the basis of Eq. (2.3) with constant coefficients. The parameters are measured with respect to C_0^k, whose value is put equal to unity. The fits push C_0^q and C_3 to the limits allowed by Eq.(2.5) and so they have here both been fixed at zero. The probabilities P of the different partial-wave configurations have typically uncertainties of $\pm 5\%$.

Q [MeV]	47.4	104.7	combined
C_0^q	0	0	0
C_0^k	1	1	1
C_1	$0.2^{+0.33}_{-0.28}$	$2.5^{+1.8}_{-0.95}$	$0.83^{+0.34}_{-0.24}$
C_2	$1.1^{+0.39}_{-0.34}$	$3.9^{+2.2}_{-1.15}$	$1.95^{+0.28}_{-0.30}$
C_3	0	0	0
C_4	$-1.9^{+0.44}_{-0.50}$	$-6.4^{+1.6}_{-3.1}$	$-3.30^{+0.38}_{-0.44}$
$P\left(\{\{K^+\bar{K}^0\}_s d\}_p\right)$	80%	79%	84%
$P\left(\{\{\bar{K}^0 d\}_s K^+\}_p\right)$	64%	72%	65%
$P\left(\{\{K^+ d\}_s \bar{K}^0\}_p\right)$	23%	16%	21%
χ^2/ndf	74.5/42	126/55	251/100

The current fits include the positivity constraints expressed by Eq. (2.5), which were not taken into account in the previous analyses [6,7]. Fortunately, the influence of these constraints on the observables is not very large and the main results are largely unaffected.

The lowest value of χ^2 would be achieved at both energies with a negative C_0^q coefficient. As shown in Eq. (2.4), C_0^q is given by absolute squares of amplitudes that cannot be negative. We therefore set $C_0^q = 0$ in the fit which, as a consequence of Eq. (2.5), means that C_3 must also vanish. The results of the combined fit to the numbers of events for different observables, corrected for chamber efficiencies, are shown in Figs.1 and 2 for the two energies.

The most obvious and striking of the results reported in Table 1 are the probabilities for the different partial-wave configurations. The $K^+\bar{K}^0$ subsystem is overwhelmingly in the s-wave, with only about 15% being in a p-wave. It is therefore clear that the $a_0^+(980)$ channel is strongly favoured in this reaction. However, it is equally evident that, since the s-wave probability for $\bar{K}^0 d$ of about two thirds is three times that for $K^+ d$, the antikaon is also strongly attracted to the baryons.

As a cross-check on the analysis, the shapes for the distributions obtained with the best global fit parameters were compared with those published in Ref. [7] and reasonable agreement was found. Since the previous analysis was done on the basis of acceptance-corrected data, the accord means that there is little ambiguity in the results originating from the uncertainties in the very non-uniform ANKE acceptance.

Figure 3 shows the differential cross sections in terms of the three two-particle invariant masses for the 104.7 MeV data compared to the results of the global fit. These acceptance-corrected $\bar{K}^0 d$ and $K^+ d$ distributions are very different, with lower masses being strongly favoured in the former case. This is even more obvious if we compare the ratio of the $\bar{K}^0 d$ to $K^+ d$ distributions which, to eliminate the effects of the kaon mass difference, is shown in Fig. 3 as a function of the mass excess $\Delta M = M_{\rm inv}(Kp) - m_K - m_p$. The ratio falls very fast with ΔM in a way that is very similar to that found for the ratio of the $K^- pp$ and $K^+ pp$ invariant mass distributions in the $pp \to ppK^+K^-$ reaction [9]. In this case the strong variation could be explained in terms of a $K^- p$ final state interaction, perhaps driven by the $\Lambda(1405)$, though it should be noted that the angular momentum constraints are far weaker there.

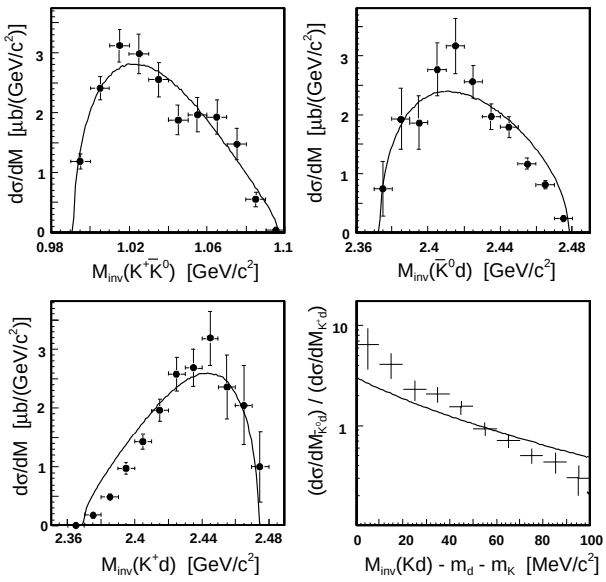

Fig. 3. Invariant mass distributions of the $pp \to dK^+\bar{K}^0$ differential cross sections at 104.7 MeV. These are compared with the constant coefficient solution of the combined fit whose parameters are given in Table 1. Also shown is the ratio of the $\bar{K}^0 d$ and $K^+ d$ distributions, plotted as a function of the mass excess $\Delta M = M_{\rm inv}(Kd) - m_K - m_d$.

Although the overall description of the $pp \to dK^+\bar{K}^0$ results shown in Fig. 3 is reasonable, it is clear that the data are lower than the fits for high $\bar{K}^0 d$ and low $K^+ d$ masses and this is particulary striking in the plot of their ratio. A more satisfactory description of these data would be achieved with a somewhat larger s-state $\bar{K}^0 d$ probability, as indicated by the single energy fit shown in Table 1. However, the disagreement may also be a reflection of the distortions introduced by the $a_0^+(980)$ resonance and the $\bar{K}^0 d$ final state interaction, to which we now turn.

4 Influence of the $\mathrm{a_0^+(980)}$ resonance and $\mathrm{\bar{K}^0 d}$ interaction in final state

Because the mass of the $a_0(980)$ resonance is very close to the $K\bar{K}$ threshold, its shape is not described satisfactorily by a Breit-Wigner form. The energy dependence of the width is taken into account in the standard Flatté parameterisation for the propagator [10]:

$$G_{a_0}(q_{K\bar{K}}) = \frac{N}{M_{a_0}^2 - m_{KK}^2 - iM_{a_0}(\bar{g}_{\pi\eta} q_{\pi\eta} + \bar{g}_{K\bar{K}} q_{K\bar{K}})}, \tag{4.1}$$

where $\bar{g}_{\pi\eta}$ and $\bar{g}_{K\bar{K}}$ are dimensionless coupling constants and very often it is their ratio $R = \bar{g}_{K\bar{K}}/\bar{g}_{\pi\eta}$ that is quoted [2]. For convenience, the normalisation constant N is chosen here such that G_{a_0} is equal to be unity at the $K^+\bar{K}^0$ threshold. The nominal mass of the resonance is M_{a_0}, $m_{K\bar{K}}$ is the $K\bar{K}$ invariant mass, and $q_{\pi\eta}$ is the $\pi\eta$ relative momentum in the a_0 rest frame. It is important to note that the relative momentum in the $K\bar{K}$ channel,

$$q_{K\bar{K}} = \tfrac{1}{2}\sqrt{m^2_{K\bar{K}} - 4m^2_K} \tag{4.2}$$

is positive imaginary below the $K\bar{K}$ threshold.

The uncertainties in the $a_0(980)$ parameters as extracted from the data collected in the different experiments are rather large, as can be seen from the compilation given in Ref. [2]. Although the statistical errors for each experiment are small, there are significant discrepancies between the quoted values of the coupling constants. This might indicate either large systematic uncertainties or be a consequence of a certain scale invariance of the Flatté parameterisation [2]. The picture is, however, little changed if one uses instead a parameterisation based on more fundamental theoretical ideas [11,12,13]. That of Achasov [11] takes into account the so-called finite-width corrections to the self-energy loop. As shown in Ref. [2], these different parameterisations are equivalent in the non-relativistic limit. To illustrate this, we show in Fig. 4 that the spectra of both Ref. [11] and Ref. [12] can be well described by a non-relativistic Flatté distribution with modified parameters. With the currently available data it is not possible to distinguish between the relativistic and non-relativistic forms.

It is to be expected that the $pp \to dK^+\bar{K}^0$ amplitudes leading to the s-wave $K^+\bar{K}^0$ final state should be modified through the introduction of Flatté propagator G_{a_0}. This effectively introduces a momentum dependence into some of the amplitudes of Eq. (2.2) and hence into the corresponding observables through Eq. (2.4).

There is also significant uncertainty in the low energy $\bar{K}d$ interaction, which is nicely summarised in Ref. [14]. The $\bar{K}d$ scattering lengths quoted there are typically

$$a_{\bar{K}d} \approx (-1.0 + i1.2)\,\mathrm{fm}\,, \tag{4.3}$$

though the spread is quite large, depending upon the theoretical assumptions and the experimental data.

In the scattering length approximation, the amplitude for the production of an s-wave $\bar{K}d$ pair should be multiplied by an enhancement factor

$$F_{\bar{K}d}(Q) = \frac{1}{(1 - iQa_{\bar{K}d})}\,, \tag{4.4}$$

which depends on the relative $\bar{K}d$ momentum Q.

5 Fit procedure and results

With the inclusion of final state interactions in both the $K^+\bar{K}^0$ and $\bar{K}^0 d$ s-wave systems, one should study the contributions indicated symbolically in Fig. 5 as well as higher order rescatterings.

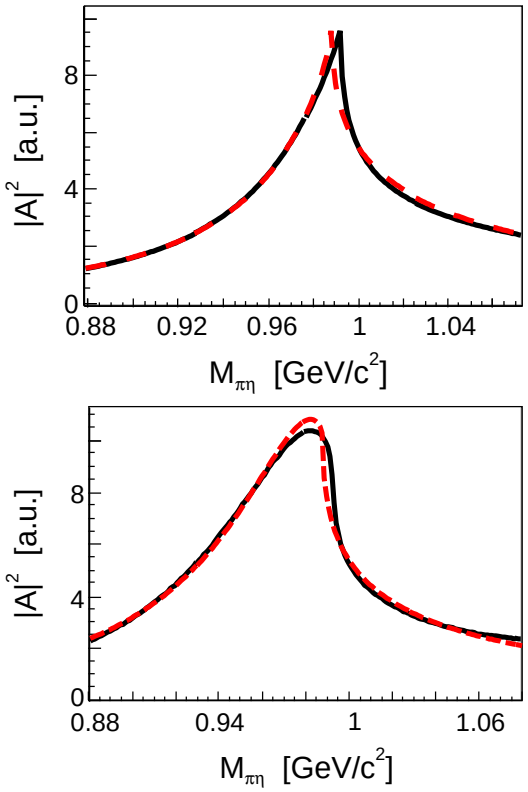

Fig. 4. Upper panel: The Achasov parameterisation (solid line) [11] compared with a non-relativistic $K^+\bar{K}^0$ Flatté function (dashed line) with the following parameters: $\bar{g}_{\pi\eta} = 0.614$, $R = 1.650$, $M_{a_0} = 1.020\,\mathrm{GeV/c^2}$. Bottom panel: The same for the Oller parameterisation [12] with following parameters: $\bar{g}_{\pi\eta} = 0.698$, $R = 1.463$, and $M_{a_0} = 0.959\,\mathrm{GeV/c^2}$.

It is important to stress at the outset that the final state interaction factors of Eqs. (4.1) and (4.4) involve unknown overall normalisations and will, at most, only describe the momentum dependence of the corresponding s-wave observable. In particular, one cannot determine the modifications to the s-wave probabilities induced by the final state interactions. For this purpose one would need full $K\bar{K}$ and $\bar{K}d$ "potentials" or their equivalent. We therefore limit ourselves here to the study of how the combined final state interactions distort the mass distributions of Fig. 4. For this we follow the procedure of Ref. [9] and assume that the final state interaction factors are multiplicative.

In principle, only the s-wave amplitudes should be multiplied by the corresponding final state interaction factor of Eq. (4.1) or Eq. (4.4). However, we have seen from Table 1 that the s waves are dominant in both the $K^+\bar{K}^0$ and $\bar{K}^0 d$ channels. We therefore make the drastic simplification of multiplying the matrix-element-squared $\langle\,\overline{|\mathcal{M}^2|}\,\rangle$ by the product of the absolute-squares of the final state interaction factors:

$$\langle\,\overline{|\mathcal{M}^2|}\,\rangle \longrightarrow \langle\,\overline{|\mathcal{M}^2|}\,\rangle \times |F_{\bar{K}d}(Q)|^2 \times |G_{a_0}(q)|^2\,. \tag{5.1}$$

This *ansatz* means that the p-waves are also modified even though there should be no final state interactions in these channels. On the other hand, the procedure avoids the introduction

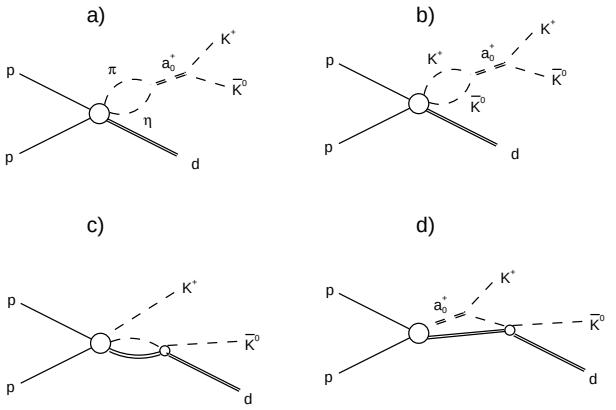

Fig. 5. Diagrams for $pp \to dK^+\bar{K}^0$ reaction: a,b) correspond to direct $a_0(980)$ production involving strong $(\pi\eta, K\bar{K})$ coupled channel effects, c) reflects non-resonant $dK^+\bar{K}^0$ production corrected by the $\bar{K}d$ final state interactions. d) includes both "rescattering" effects.

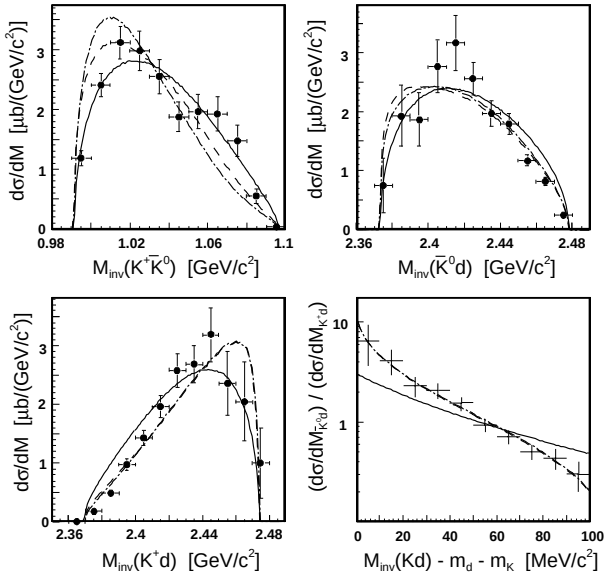

Fig. 6. Invariant mass distributions of the $pp \to dK^+\bar{K}^0$ differential cross sections at 104.7 MeV compared with predictions of the combined fit, where *fsi* distortions are introduced using the *ansatz* of Eq. (5.1) with the Bugg *et al.* [16] (dashed curve) and Teige *et al.* [15] (chain curve) parameterisations of the $a_0^+(980)$. The results of the constant amplitude approach of Fig. 3 are presented for orientation (solid line). The fit to the ratio of the $\bar{K}^0d$ and K^+d distributions is insensitive to the parameters of the $a_0^+(980)$.

of extra parameters that depend upon the relative phases of the s and p waves.

A new combined fit to the two data sets was undertaken on the basis of the *ansatz* of Eq. (5.1), and the results for the invariant mass distributions at 104.7 MeV are shown in Fig. 6 for both the Bugg *et al.* [16] and Teige *et al.* [15] parameterisations of the $a_0^+(980)$ which correspond, respectively, to a wide and narrow resonance. The $K^+\bar{K}^0$ spectrum is better described when the wider $a_0^+(980)$ is used but the major improvement seen from the introduction of these distortions is in the $\bar{K}^0/K^+$ ratio, where the excellent description depends relatively little on the parameters chosen for the $a_0^+(980)$ resonance and almost entirely upon the $\bar{K}^0d$ *fsi*.

Owing to the relatively small phase space volume, the data at 47.4 MeV are not sensitive to the $a_0^+(980)$ parameters (Fig. 7). The ratio of the $\bar{K}^0d$ and K^+d distributions is enhanced at the low mass region. However, this enhancement is weaker than the result of the fit which is based on Eq. (5.1).

At low energies both the $K^+\bar{K}^0$ and $\bar{K}^0d$ systems must be in regions where the cross section is enhanced by the two *fsi*. As a consequence, the total cross section predicted using the *ansatz* of Eq. (5.1) shows a slower energy variation than when the constant coefficients are used. This is seen clearly in Fig. 8, where the results at the two measured energies [6, 7] are compared with predictions that are normalised to the 104.7 MeV point.

The introduction of either *fsi* increases the cross section at the lower energy by a similar amount and the inclusion of both effects improves significantly the agreement with the 47.4 MeV point.

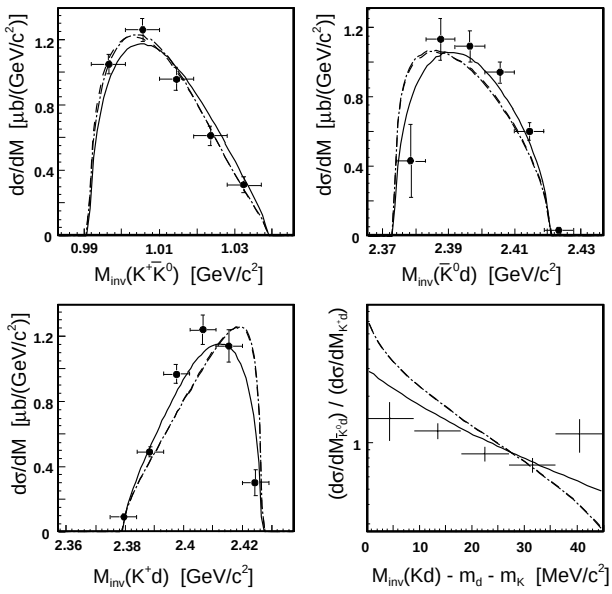

Fig. 7. As for Fig. 6 but at an excess energy of 47.4 MeV.

6 Conclusions

We have presented a combined analysis of the measurements of the $pp \to dK^+\bar{K}^0$ reaction made with the ANKE spectrometer at COSY at excess energies of 47.4 and 104.7 MeV. The application of the Pauli principle, combined with the conservation of angular momentum and parity, shows that an overall s-wave is forbidden in the final state. There must be at least one p or higher wave. The data clearly demonstrate that both the $K^+\bar{K}^0$ and $\bar{K}^0d$ systems are dominantly in s-waves, while p-waves dominate the K^+d channel. The big difference between the kaon and antikaon interactions with the deuteron is seen most clearly in the ratio of the differential cross sections in terms of the Kd invariant mass. This ratio seems to depend pri-

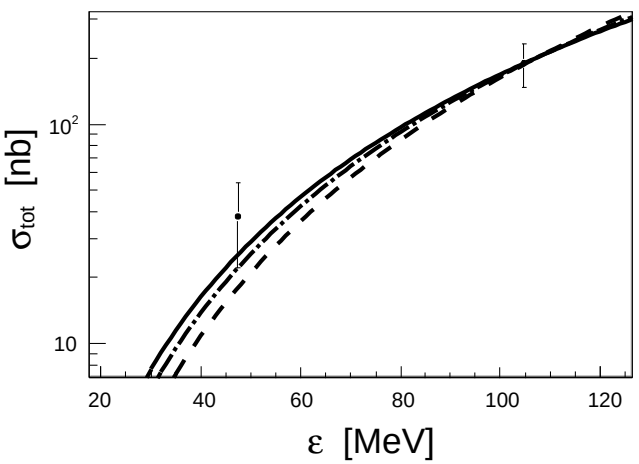

Fig. 8. Total cross section for the $pp \to dK^+\bar{K}^0$ reaction as a function of the excess energy ϵ. Points with errors are the cross sections measured with the ANKE spectrometer [6,7]. The dashed line, which is normalised on the 104.7 MeV point, shows a phase space simulation with the fixed partial wave contributions, as defined by the joint fit of Table 1. The solid line shows the corresponding energy dependence after the introduction of the *fsi* in both the $a_0^+(980)$ and $\bar{K}d$ channels. The inclusion of either the $a_0^+(980)$ or $\bar{K}d$ alone leads to almost identical results, which are shown by the chain curve.

marily on the $\bar{K}d$ interaction. The fast variation observed there is similar to that found in the K^-pp/K^+pp ratio measured in the $pp \to ppK^+K^-$ reaction.

The effects of the $a_0^+(980)$ scalar resonance are more subtle, though the fact that the $K^+\bar{K}^0$ is almost entirely in an s-wave is a strong indication of its influence. The shapes of the differential distributions are little changed from those of the constant parameter solution provided that both the $\bar{K}^0d$ and $K^+\bar{K}^0$ final state interactions are taken into account. It is then clear that the $a_0^+(980)$ *fsi* compensates the $\bar{K}^0d$ distortion of the $K^+\bar{K}^0$ spectrum so that there is a delicate interplay between these two *fsi*. More theoretical work is clearly necessary here to get a fuller understanding and attempts have been made to study this problem on a more fundamental level [20].

The two final state interactions taken together enhance the ratio of the total cross section $\sigma(47.4\,\mathrm{MeV})/\sigma(104.7\,\mathrm{MeV})$ and lead to a better description of the published data. Within the framework of the simple approach presented here, even greater sensitivity would be achieved if we had total cross section data closer to threshold.

The authors would like to thank many of the other members of the ANKE collaboration for discussions and especial mention here should go to V. Grishina, L. Kondratyuk, and A. Sibirtsev. This work has partially been supported by BMBF, DFG, Russian Academy of Sciences, and COSY FFE.

References

1. E. Klempt and A. Zaitsev, Phys. Rept. **454** (2007) 1.
2. V. Baru *et al.*, Eur. Phys. J. A **23** (2005) 523.
3. V. Baru *et al.*, Phys. Lett. B **586** (2004) 53.
4. D. V. Bugg, Eur. Phys. J. C **47** (2006) 57.
5. M. Büscher *et al.*, Nucl. Instr. Methods A **481** (2002) 378.
6. V. Kleber *et al.*, Phys. Rev. Lett. **91** (2003) 172304.
7. A. Dzyuba *et al.*, Eur. Phys. J. A **29** (2006) 245.
8. C. Hanhart, Phys. Rept. **397** (2004) 155.
9. Y. Maeda *et al.*, Phys. Rev. C **77** (2008) 015204.
10. S. Flatté, Phys. Lett. B **63** (1976) 224.
11. N. N. Achasov, A. N. Kisilev, Phys. Rev. D **68** (2003) 014006.
12. J. A. Oller, E. Oset, Nucl. Phys. A **652** (1999) 407.
13. D. R. Boito and M. R. Robilotta, Phys. Rev. D **76** (2007) 094011, arXiv:0705.3260 [hep-ph]; E. van Beveren and G. Rupp, arXiv:0706.4119 [hep-ph]; F. Giacosa and G. Pagliara, Phys. Rev. C **76** (2007) 065204, arXiv:0707.3594 [hep-ph].
14. U.-G. Meißner, U. Raha, A. Rusetsky, Eur. Phys. J. C **47** (2006) 473, arXiv:nucl-th/0603029.
15. S. Teige *et al.*, Phys. Rev. D **59** (1999) 012001.
16. D.V. Bugg *et al.*, Phys. Rev. D **50** (1994) 4412.
17. A. Abele *et al.*, Phys. Rev. D **57** (1998) 3862.
18. A. Aloisio *et al.*, Phys. Lett. B **536** (2002) 209.
19. M. N. Achasov *et al.*, Phys. Lett. B **479** (2000) 53.
20. E. Oset, J. A. Oller and U.-G. Meißner, Eur. Phys. J. A **18** (2003) 343.